Quality Technology &
Quantitative Management
Vol. 3, No. 3, pp. 263-282, 2006

QTQM

Multiscale Statistical Process Control of Paper Surface Profiles

Marco S. Reis and Pedro M. Saraiva

Department of Chemical Engineering, University of Coimbra, Coimbra, Portugal
(*Received* February 2005, *accepted* September 2005)

Abstract: Paper surface plays a key role in paper quality. Accurate paper surface profiles contain the fundamental raw information of the surface for a wide range of length-scales, to which different aspects of the paper quality are connected. With the goal of exploring the availability of such paper surface data obtained through a mechanical stylus profilometer, we present in this paper an approach for setting up a Multiscale SPC procedure that monitors simultaneously two key quality surface phenomena that develop at different scales: roughness and waviness. The raw profiles, after adequate processing using a multiscale framework based on wavelets, give rise to quantities that can be effectively used to monitor these two phenomena in a simple and integrated way, and therefore be implemented in practice for quality control purposes. The effectiveness of the proposed procedure is assessed by simulation as well as through a pilot study involving real paper surface profiles.

Keywords: Multiscale analysis, paper surface, process monitoring and diagnosis, statistical process control, wavelets.

1. Introduction

Paper is a very complex material, exhibiting properties that derive from a structural hierarchy of arrangements for different elements (molecules, fibrils, fibres, network of fibres, etc.), beginning at a scale of a few nanometres and proceeding all the way up to a few dozens centimetres or even meters [20]. This complexity is also present at its boundary, the paper surface, which plays a central role in many of the relevant properties from the perspective of the end user, such as general appearance (optical properties, flatness, etc.), printability (e.g. the absorption of ink) and friction features, to name a few. Being aware of this importance, the Pulp and Paper Industry developed methods to assess and characterize paper surface features at different scales, and, in particular, special attention has been devoted to surface phenomena known as *roughness* and *waviness*. Roughness is a fine length-scale phenomena, that results from the superposition of the so called optical roughness (scales up to $1\mu m$), micro roughness (scales between $1\mu m-100\mu m$) and macro roughness (scales between $0.1mm-1mm$), each one with their own specific structural elements [18]. It is usually characterized indirectly by instruments based upon the air-leakage principle, quite handy and fast for integration in production quality control schemes, but also somewhat uninformative regarding the nature of the irregularities that drive this phenomenon. Waviness, on the other hand, refers to those larger scale deviations from a flat shape, an example of which are the so called "piping streaks", that consist of streaks aligned along the largest dimension of paper, 1-3 *cm* wide, that may develop as a consequence of different fibre alignment streaks across the paper machine [37], but other representatives do exist, including the so called "flutes/ fluting" in heavy ink coverage areas [31], and cockling, which consists of small "bumps", 5-50 *mm* in diameter, occurring at random positions in the sheet as a consequence of hygroexpansivity and structural unevenness of paper [23], [18]. Quite often these larger scale waviness phenomena are assessed by trained operators through subjective classification schemes based upon sensorial analysis using several criteria defined *a priori* by a panel of experts, but efforts have also been carried out towards the development of more systematic and instrumental-based methodologies, namely using optical technology [31] and mechanical stylus profilometry [8]. Profilometry, in particular, is a technique that collects a detailed profile of the paper surface, to be processed afterwards in order to calculate several parameters that summarize the main features of the profile at a given range of scales where the analysis is to be focused. The complete surface profiles contain all the raw information necessary to characterize the phenomena located at different scales, ranging from a few micrometers to a few centimetres [42]. Figure 1 presents the raw data for a real paper profile, and its decomposition into components relative to different scales. These components result from a multiscale decomposition followed by a selective aggregation of scales made in order to isolate the two main surface phenomena that we want to monitor (roughness and waviness), as will be described in Section 3.

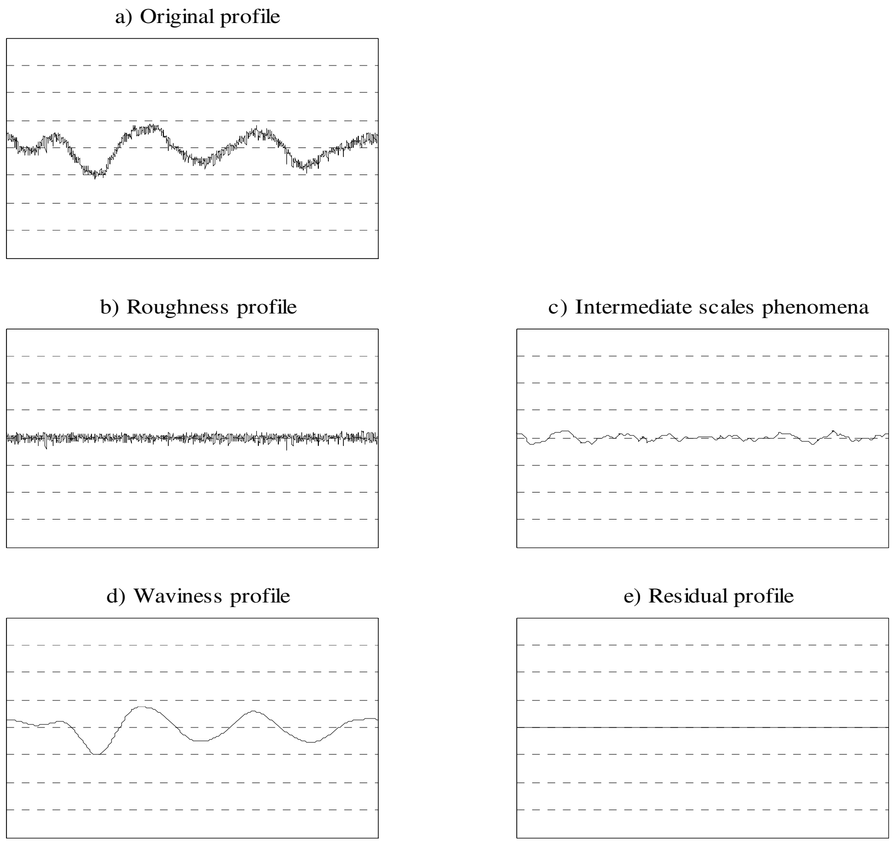

Figure 1. The original profile (a) and the associated surface phenomena located at different scales, obtained by performing a multiscale decomposition based on the wavelet transformation followed by scale aggregation using accumulated engineering knowledge: b) roughness profile; c) intermediate scales phenomena, that will not be used in this work for monitoring purposes; (d) waviness profile; and (e) residual profile. Summing up the last four profiles (b-e), one obtains the original measured surface profile (a).

Our aim in this work is to take advantage of such types of raw data (along with an adequate decomposition framework) to set up a Statistical Process Control scheme that addresses directly the fundamental nature of irregularities related to each phenomenon and not to some indirect or subjective measure of them.

The issue of monitoring process and product profiles is not new, and has been recently brought to the attention of the scientific community [44], as being "the most promising area of research in statistical process control". In this reference, work carried out in applications involving linear and non-linear profiles (using splines and wavelets) is reviewed, along with discussions regarding both Phase I and Phase II methodologies. Profiles monitoring is also a well established reality in the field of monitoring batch processes. In such a context, profiles regard data collected during the progress of the batch, and methodologies such as principal components analysis, partial least squares and several multiway analysis frameworks have been proposed and used with success [30,29,43]. The chemometrics community has also developed techniques to process profiles arising from spectra collected using several sources (e.g., NIR), some of which with the goal of process monitoring [33], and, more recently, similar applications involving the use of images (an higher dimensional profile) have also been reported [4].

As to paper itself, the surface profiles present a multiscale structure and the phenomena we want to monitor, roughness and waviness, indeed arise at different length-scales. This so called multiscale data, in opposition to data that can be thoroughly characterized using a single scale (of time or length), can be very adequately handled using frameworks based upon wavelet theory. Wavelet-based methodologies do enable the incorporation of the concept of scale right into the core of data analysis, thus providing an adequate mathematical language to describe multiscale phenomena. In fact, there is already a quite extensive list of papers reporting application of wavelets in process monitoring schemes, that somehow explore the decorrelation and energy compaction ability of the wavelet transform [2,10,41], in the improved detection of underlying deterministic events immerse in a stochastic, possibly autocorrelated background. Both the univariate [2,38] and multivariate cases [1,19,27] have been addressed, as well as non-linear applications [12,35]. Ganesan et al. [13] present a review paper, where over one hundred and fifty papers are cited regarding multiscale monitoring. In this context, several developments have also been reported regarding applications to profile monitoring. Trygg et al. [39] applied a 2D wavelet transformation to compress data from NIR (near-infrared) spectra collected over time and estimated a PCA model for this 2D compressed matrix, that was then used to check whether new incoming spectra deviate from those collected during normal operation. Other applications to process monitoring of profiles based on wavelet coefficients and metrics derived from it, include the following: quadropole mass spectrometry data from rapid thermal chemical vapour deposition process [21], tonnage signals from a stamping process [16,17], the central azimuth curve of antenna signals [15], print mottle images [3] and unprinted paper images [5] to assess paper quality regarding its printing performance and formation (i.e., the degree of uniformity in the fibre network that constitutes paper), respectively, data from a semi-batch copolymerization process [45] and electrochemical noise data (fluctuation in potential) to characterize localized corrosion processes [9].

Paper surface profiles do present, however, some characteristics that make them different from those analyzed in the applications reported in the literature referred above. Since the sample to be analyzed is collected at random, the location of a given feature in the length direction (X-axis) is not very critical but the global behaviour of the profile obtained for the relevant scales is. Furthermore, paper surface does present a multiscale structure linked to a physical, and in fact observable, reality, which enables the gathering of engineering knowledge, that can be then applied to the selection of those scales that are of interest for each particular surface phenomenon we want to address.

In the following section, we present a brief summary of wavelet theory, that plays a central role in our monitoring methodology, to be presented in the third section. Then, in section 4, we test the suggested multiscale monitoring methodology using both computational simulations and real data from paper surface profiles acquired using a mechanical stylus profilometer. We also present at this point a diagnostic extension that enables a finer characterization of a significant event in the waviness control chart, conceived to assist operators once a special event of this type is detected. A conclusions section sums up the proposed methodology and results obtained.

2. Wavelet Transformation and Multiscale Decomposition

In general terms, a transform provides an alternative and equivalent way of representing raw data as an expansion of basis terms multiplied by the transform coefficients. These coefficients constitute the "transform" and, if the methodology is properly chosen, data analysis can become much more efficient and effective when conducted over them, instead of over the original data set. For the particular class of signals exhibiting complex multiscale features, i.e. patterns appearing at different *locations* and with different *localizations* either in time or frequency [2], the usual linear transforms, such as the Fourier transform, do require a large number of high magnitude coefficients to reproduce them, and therefore do not provide a very efficient representation. This happens because the form of the time/ frequency windows [25, 41] associated with their basis functions does not change across the time/ frequency plane, in order to cover effectively and efficiently the localized high energy zones of the several features present in the signal. Wavelet basis, on the other hand, do provide an alternative coverage of this plane that is especially adequate to handle such type of signals (the so called "constant-Q" scheme, [32]).

Wavelets are a particular type of functions whose location and localization characteristics in time/ frequency are ruled by two parameters: both the *localization* in this plane and the *location* in the frequency domain are determined by the scale parameter, *s*, whereas the *location* in the time domain is controlled by the time translation parameter, *b*. Each wavelet, $\psi_{s,b}(t)$, can be obtained from the so called "mother wavelet", $\psi(t)$, through a scaling operation (that "stretches" or "compresses" the original function, establishing its form) and a translation operation (that controls its positioning in the time axis):

$$\psi_{s,b}(t) = \frac{1}{\sqrt{|s|}} \psi\left(\frac{t-b}{s}\right). \tag{1}$$

The shape of the mother wavelet is such that it does have an equal area above and below the t – axis, satisfying the following equation:

$$\int_{\mathbb{R}} \psi(t)\,dt = 0\,. \tag{2}$$

As a result, besides having a compact localization in this axis, wavelets do also oscillate around it, feature from which derives the name of "wavelets" (small waves). The mother wavelet also presents an unit norm:

$$\int_{\mathbb{R}} \psi^2(t)\,dt = 1 . \tag{3}$$

In Continuous Wavelet Transforms (CWT), the scale and translation parameters vary continuously, constituting a redundant transformation. Therefore, in order to construct a basis set, these parameters should be appropriately sampled, so that the set of wavelet functions parameterized by the new indices (scale index, *j*, and translation index, *k*) does cover the time-frequency plane in a non-redundant way. This sampling consists of applying a dyadic grid in which *b* is sampled more frequently for lower values of *s*, and *s* grows exponentially with the power of 2:

$$\psi_{j,k}(t) = \psi_{s,b}(t)\Big|_{\substack{s=2^j \\ b=k\cdot 2^j}} = \frac{1}{2^{j/2}}\psi\left(\frac{t-k\cdot 2^j}{2^j}\right) = \frac{1}{2^{j/2}}\psi\left(\frac{t}{2^j}-k\right). \tag{4}$$

Mallat [24] presented a multiscale (or multiresolution) decomposition framework, where coarser approximations of a given signal represented at the finest scale can be considered as projections to approximation subspaces V_j indexed by scale index *j*, that span progressively shorter regions of $L^2(\mathbb{R})$, and have a nested structure ($V_{j+1} \subset V_j$, $V_{j+1} \neq V_j$). On the other hand, details that are lost in this process of projecting the signal to increasingly coarser approximation spaces can also be considered as projections to complementary subspaces, the details spaces, W_j, that, in conjunction with the approximation space, span the space of the original signal. In other words, this allows us to write a given signal at the finest scale, say $f_0(t)$, as the sum of its projection to the approximation space at scale *j*, plus all the details relative to the scales in between:

$$f_0(t) = f_j(t) + \sum_{i=1}^{j} w_i(t) \Leftrightarrow f_0(t) = \mathrm{Pr}_{V_j} f_0(t) + \sum_{i=1}^{j} \mathrm{Pr}_{W_i} f_0(t) . \tag{5}$$

The projections $f_j(t)$ and $\{w_i(t)\}_{i=1,\ldots,j}$ in (5) can adequately be written in terms of linear combinations of the spaces basis functions multiplied by the expansion coefficients (calculated as inner products of the signal and the basis functions). These expansion coefficients are called approximation coefficients, a_k^j $(k \in \mathbb{Z})$, and details coefficients, d_k^i $(i = 1,\ldots, j;\ k \in \mathbb{Z})$, and are usually referred to as the (orthogonal) Discrete Wavelet Transform [7] or simply as "wavelet coefficients", Equation (7). The basis functions of the approximation space V_j are the so called "scaling functions", $\{\phi_{k,j}(t)\}_{k\in\mathbb{Z}}$, that, similarly to what happens with wavelets, can be generated from $\phi(t)$ (also known as "father wavelet") by appropriate scaling and translation operations. The $\phi(t)$ function is also constrained to unit norm:

$$\int_{\mathbb{R}} \phi^2(t)\,dt = 1 . \tag{6}$$

$$f_0(t) = \sum_k a_k^j \phi_{j,k}(t) + \sum_{i=1}^{j}\sum_k d_k^i \psi_{i,k}(t) ,\ a_k^j = \left\langle f_j(t), \phi_{j,k}(t)\right\rangle,\ d_k^i = \left\langle f_j(t), \psi_{i,k}(t)\right\rangle . \tag{7}$$

The basis functions for the detail spaces are the already presented wavelet functions. When working with discrete data (such as is the case with surface profiles) the procedure adopted consists of assuming that such signals constitute already the projection onto the approximation space V_0, which means that its values coincide under this circumstances with a_k^0 $(k \in \mathbb{Z})$. Then, the expansion coefficients presented in Equation (7) are computed by applying the highly efficient recursive procedure proposed by Mallat [24], with a computational complexity $O(N)$.

Using these concepts and terminology, we can now interpret more thoroughly what is being portrayed in Figure 1: (a) is the original (sampled) signal, f_0; (b) is the roughness profile, given by the sum of the projections of f_0 onto the detail spaces with scales allocated to the roughness phenomena, $R = \sum_{i \in J_{Rog}} w_i$; (c) is the intermediate scales phenomena profile, given analogously by $IS = \sum_{i \in J_{IS}} w_i$; (d) is the waviness profile, given by $W = \sum_{i \in J_{Wav}} w_i$; and finally (e) is the residual profile, given by the projection of f_0 onto the approximation space at the coarsest scale J , f_J , which is also the decomposition depth used for analysing our profiles. In particular, the index sets for the scales relative to each phenomenon are defined by $J_{Rog} = \{1,2,\ldots,6\}$ (roughness), $J_{IS} = \{7,8,9\}$ (intermediate scales) and $J_{Wav} = \{10,11\}$ (waviness), as results from both engineering knowledge and a careful analysis of profiles, to be discussed in the next section.

3. A Multiscale SPC Approach for Monitoring Paper Surface Phenomena

3.1. The Proposed Framework

The proposed approach for conducting integrated Multiscale SPC (MS-SPC), in order to monitor both roughness and waviness phenomena simultaneously, has the following basic components:

1. Acquisition of a paper profile on a predefined direction.
2. Multiscale decomposition of the de-trended profile (i.e., the profile with linear trend removed), obtaining the wavelet coefficients at each scale ($j = 1 : J$, where J is the decomposition depth).
3. Using only those scales whose indices are relative to roughness and waviness phenomena (sets J_{Rog} and J_{Wav}), calculate the parameters that summarize the relevant information for product quality control purposes (this may require the separate reconstruction of these two profiles back into the original domain, by applying the inverse wavelet transform to a set of processed coefficients where the only non-zero elements are those corresponding to the selected scales for each phenomenon). Examples of this type of parameters are, for instance, the variance of the detail coefficients at a certain scale, or the maximum profile valley depth [14] of the reconstructed profiles.
4. Implementation of SPC procedures for monitoring the parameters calculated in step 3.
5. If an alarm is produced, we check for its validity and look for root causes when appropriate. If it occurs in the waviness control chart, we use a diagnostic tool to characterize the event more fully (see below). Otherwise, return to step 1, and repeat the whole procedure for the next paper sheet profile acquired.

3.1.1. Acquisition of Profile

The measurement device that we use for step 1 is a MahrSurf mechanical stylus profilometer set, with a Perthometer S2 data processing unit, a drive unit PGK 120, and a MFW – skidless pick-up set. The profiles to be processed contain the central 6144 measures of surface height, separated by approximately $8.93\ \mu\text{m}$, taken in the paper cross direction, as the type of waviness phenomena we are especially concerned with, the "piping streaks", do always occur along a direction that is perpendicular to the measured one. Thus, using cross direction paper profiles, we can assess the magnitude of cross direction roughness together with that of "piping streaks" (as illustrated in Figure 1a). Furthermore, other large scale deformations, without any directional preferential alignment, such as "cockling", can also be detected.

3.1.2. Wavelet Decomposition

The decomposition depth used in step 2 is $J = 11$, so that the frequency range where "piping streaks" do develop can be adequately covered. An orthogonal Symmlet-8 wavelet filter [25] was employed, since: the shape of its associated wavelet does resemble that of waviness profiles; it is smooth; does have a compact support; and is more symmetric (by design) then filters from the Daubechies orthogonal wavelet family.

3.1.3. Selection of Scales Relative to Each Phenomenon

As already mentioned, engineering knowledge refers that roughness scales range up to 1 *mm*, meaning that the maximum scale index should be somewhere between 6 and 7 (because, $10^{-3} m \in \left[2^6, 2^7\right] \times 8.93 \times 10^{-6} m$). On the other hand, by carefully analysing the multiscale patterns for different metrics in several profiles with different waviness magnitudes, but approximately the same roughness behaviour, and, in particular, if we look at the variance of the detail coefficients at each scale (Figure 2), we clearly detect a change of pattern occurring slightly before scale 6, indicating that roughness phenomena stop somewhere between scales 4 and 6.

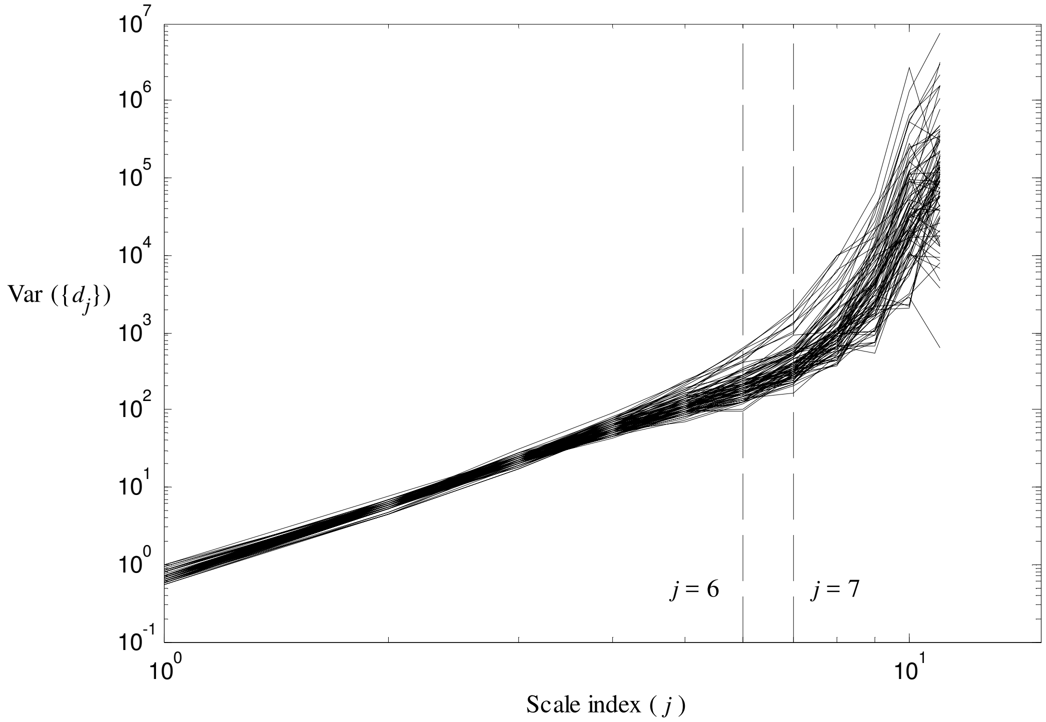

Figure 2. Log-log plot of the variance of detail coefficients at each scale (*j*), for 90 surface profiles taken in the paper cross direction. These samples have different levels of waviness magnitude, but similar roughness behaviour.

Therefore, balancing these two pieces of information, we set the maximum scale index for roughness phenomena equal to 6, as an adequate compromise between the engineering knowledge available about this particular phenomenon and the analysis performed on a selected group of samples. The scale indices associated with this phenomena are then as follows: $J_{Rog} = \{1, 2, \ldots, 6\}$. As to those relative to waviness, the maximum scale index is limited by the decomposition depth scale (11), and we set the minimum scale index equal to 10, in order to capture the minimum scale associated with "piping streaks" surface irregularities, since: $2^{10} \times 8.93 \times 10^{-6} m \approx 0.01 m \ (1 cm)$. Thus, the scale indices adopted for monitoring waviness phenomena are $J_{Wav} = \{10, 11\}$.

Another task to be performed in step 3 regards the calculation of parameters that summarise the relevant characteristics of the two phenomena to be employed for quality control purposes. Many metrics have been proposed to characterize both roughness (e.g. arithmetical mean deviation of profile, maximum height of profile, RMS deviation of profile, etc.) and waviness profiles (e.g. total height of profile, mean width of profile elements, slope of profile, etc.), that can be consulted in the profilometry literature [34] and norms [14], to which we can sum up others based upon wavelet coefficients (e.g. variance of detail coefficients distributed across selected scales for each phenomenon, and its slope in a log-log plot for roughness scales). As many of these metrics give rise to highly correlated data sets when used together, we can either use them all and compress the monitoring dimension space using, for instance, PCA, or choose a subset that provides all the important profile information for monitoring purposes, and set up control charts only for this subset. Using extended simulations and analysing real data profiles, we verified that very often a single adequately chosen parameter is good enough to detect magnitude changes in the roughness and waviness phenomena. This parsimonious solution works quite well, but can also be easily extended to incorporate more parameters. Therefore, the parameter (*statistic*, in the usual statistical terminology) chosen for monitoring roughness is the sample or empirical variance of the reconstructed roughness profile:

$$\textit{Empirical variance of roughness profiles} = \frac{\sum_{k=1}^{N} \left(R_k - \bar{R} \right)^2}{N-1}, \tag{8}$$

where $R \equiv \{R_k\}_{k=1:N}$ is the roughness profile (N stands for the number of points in the roughness profile, which is also the same as the length of the original profile), obtained by performing an inverse wavelet transformation of the vector of wavelet coefficients where the only non-zero elements are those relative to the roughness scales, or, equivalently, $R = \sum_{i \in J_{Rog}} w_i$, $\bar{R}$ corresponds to its sample average (note that both the roughness profile, R, and the projections to the detail spaces, w_i, are vectors of the same dimension, N). As for the chosen waviness parameter (once again a statistic under the usual statistical terminology), we defined a simple magnitude parameter that correlated quite well with the visual assessment of waviness profiles, given by the maximum deviation from the mean value, $D_{\max}$, defined as:

$$D_{\max} = \max\left(C_p, C_v \right), \tag{9}$$

where C_p and C_v represent, respectively, the largest peak height and the largest valley depth of the profile centred at its mean value, $C(x) = W(x) - Z_m$, where Z_m is defined as:

$$Z_m = \frac{1}{x_{\max} - x_{\min}} \int_{x_{\min}}^{x_{\max}} W(x)dx \ , \tag{10}$$

i.e., $C_p = \max(C(x))$ and $C_v = \min(C(x))$ ($x_{\min}$ and $x_{\max}$ represent the initial and final X-axis coordinates, to be considered for the purpose of calculating Z_m); W is the waviness profile, obtained through the same procedure adopted for R, but using the waviness scales instead in the reconstruction algorithm: $W = \sum_{i \in J_{Wav}} w_i$.

3.1.4. Implementation of SPC Monitoring

The two parameters referred above are used to monitor the multiscale phenomena in step 4, through two separate Shewhart control charts for individual observations [28]. Its upper control limits were set through a non-parametric approach, using a Gaussian kernel density estimation methodology [36] over reference data that do correspond to normal operation conditions. As the underlying reference distribution depends strongly upon real industrial production conditions, and since no sufficient data are available at the moment to describe it thoroughly using a parametric approach, this alternative allowed us to assess the potential utility of our methodology. Furthermore, other SPC procedures can also be implemented in the future, such as CUSUM or EWMA, to enhance sensitivity to small shifts, as extensions of the proposed approach.

In step 5 we provide the operator with a diagnosis tool that maps each waviness profile into a two dimensional plot of $\lambda_{\max}$ versus $D_{\max}$, where $\lambda_{\max}$ stands for the finite wavelength where power spectra reaches a maximum. Since "piping streaks" are well localized in the frequency domain (they have a characteristic wavelength typically somewhere around 20 *mm*, but this value depends upon a specific paper machine), this plot allows for the fast identification of those high magnitude samples that may be classified into this type of abnormality. Several reference horizontal lines assist operators in the classification of the magnitude of the phenomena into three quality classes (good, intermediate, bad), which reflect the perception of a panel of experts, being afterwards translated into values of $D_{\max}$. Another vertical reference line provides a separation between two wavelength ranges, one of which regards the "piping streaks" characteristic wavelength domain (Figure 7).

3.2. A Short Discussion of the Proposed Approach

As the monitoring parameters (or statistics) were calculated from the roughness and waviness profiles obtained upon reconstruction back into the original domain of the respective wavelet coefficients, our methodology essentially consists of a multiscale filtering procedure to separate relevant phenomena occurring at different scales. This could also be done using frequency domain techniques, which, in fact, constitute the currently adopted approach, where profiles are separated using high and low-pass filtering techniques with normalized wavelength cutoffs [14,34]. However, there are some advantages of adopting a multiscale approach. For instance, in the context of the spectral analysis of paper profiles using frequency based techniques, Wågberg and Johansson [42] refer that plotting the power spectrum over relative bands instead of linear bands would facilitate the extraction of contributions arising from different parts of the spectrum, suggesting an octave series as an adequate one. This is just the way information is organized across the scales obtained through the wavelet transform, and, in fact, we have already used this property for analysing the range of scales where roughness phenomena dominate the profile structure (Figure 2). Furthermore, multiscale methods address multiscale phenomena using an adequate mathematical language, i.e., using the concept of scale as the core of the analysis, instead of frequency, more connected to periodic phenomena. This facilitates the analysis and interpretation of results, and moves the discussion towards the very nature of the underlying phenomena. On the other hand, the availability of well established multiscale tools allows one to quickly visualize and quantify any structure at a given scale, without having to worry with the non-trivial problem of selecting the adequate cutoffs and filtering procedures, but only with the selection of the scales to consider, something much closer to our physical perception of the problem, and thus easier to use.

4. Application of the MS-SPC Approach for Monitoring Paper Surface Phenomena

In this section we test our MS-SPC procedure for the simultaneous monitoring of paper roughness and waviness, using several simulated scenarios as well as real industrial data. In the simulations, realistic paper surface profiles were generated, representing a variety of situations that go from typical normal operating conditions to several degrees of abnormal situations (moderate and high), in order to evaluate the sensitivity of the proposed methodology to shifts, and therefore its potential adequacy for real world industrial practice. Then, using real paper surface profiles, we tested how the methodology performs in practice through a set of approximately one hundred cross direction paper surface profiles representing mainly different levels of waviness magnitude, but where some abnormal roughness behaviour can also be found.

4.1. Monte Carlo Simulation Study

This simulation study regards an assessment of the underlying potential of our MS-SPC methodology under simulated, though realistic, scenarios. As the behaviour of the true underlying industrial process, and therefore that of the monitoring statistics, are both rather complex and, to a larger extent, remain unknown at the present stage, we present here results that can be used to evaluate such a potential, deferring the accurate characterization of its Phase 2 performance (e.g., through ARL, ATS metrics) to future work, when sound statistical modelling becomes possible with the availability of larger data sets.

To design a realistic simulation study, both waviness and especially roughness phenomena were carefully analysed, in order to estimate adequate models that are compatible with the main features present in real world paper surface profiles. This means that, for instance, the simulated roughness profiles should exhibit a power spectrum compatible with the results presented in Figure 2, which renders some descriptions from the field of statistical geometry of random fibre networks, that lead to simple *iid* Normal or Poisson models with high mean value [18] inadequate, as they do not give rise to power spectra with such characteristics (they lack the autocorrelation modelling arising from the natural dependencies between the measurements of height in adjacent positions). On the other hand, analysing the height distributions in roughness profiles we often found distributions slightly skewed towards the left, as happened also with other authors [11]. Therefore, in order to develop a model for the (cross direction) roughness of the paper grade that we want to describe (R), we adopted an approach based on time series theory [6,22], and fitted a suitable autoregressive moving average model (ARMA) that reproduces observed characteristics of roughness. In this regard, ARMA(2,2) was found to be the lowest order model that passes both the residual autocorrelation and partial-autocorrelation tests. From all the normal operation roughness profiles, we choose a typical one to fit ARMA model parameters, making sure that these parameters do represent the overall set of models obtained from fitting all the available normal operation roughness profiles. The model thus obtained is as follows:

$$\begin{aligned} & A(q)W(t) = C(q)e(t), \text{ with} \\ & A(q) = 1 - 0.6605q^{-1} - 0.09479q^{-2} \\ & C(q) = 1 + 0.8111q^{-1} + 0.2365q^{-2} \\ & e(t) \sim iid\, N\left(0, \sigma_e^2\right), \ \sigma_e^2 = 2.3320 \end{aligned} \tag{11}$$

where $A(q)$ and $C(q)$ are polynomials in the shift operator, q, such that $q^{-1}W(k) = W(k-1)$. Figure 3 illustrates the validity of the estimated model regarding a description of the true raw profile, in terms of the sample autocorrelation and partial-autocorrelation functions. We also verified that it reproduces the desired power spectrum behaviour within the roughness scales range.

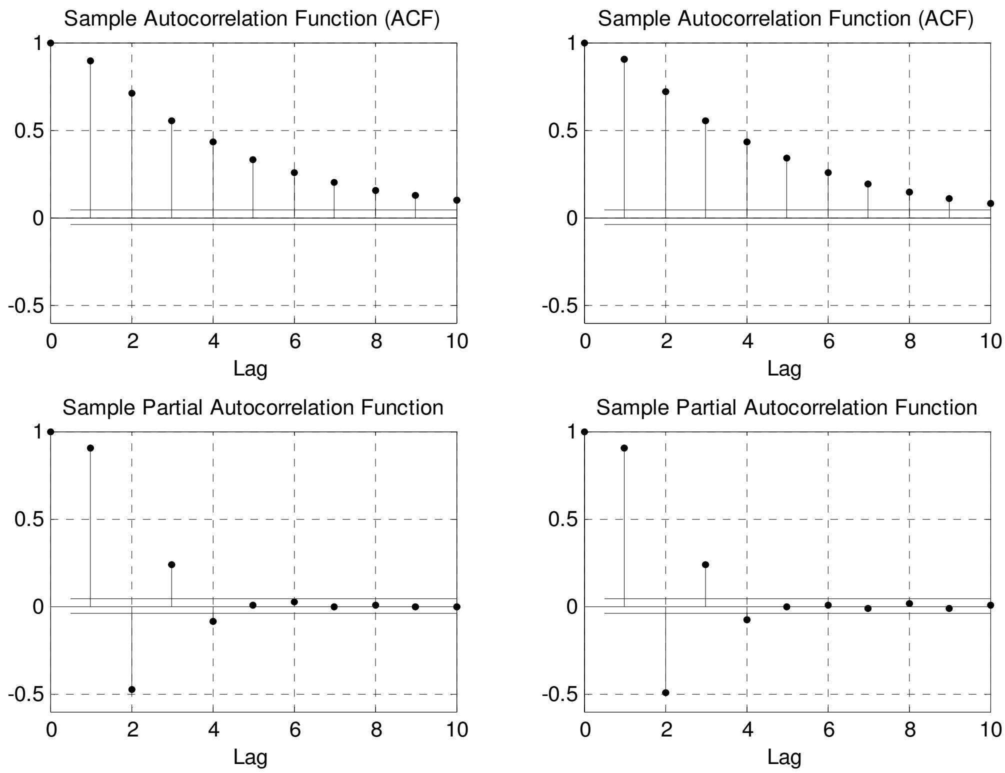

Figure 3. Sample autocorrelation and partial autocorrelation functions for a real roughness profile (left) and for a simulated profile using the estimated model (right).

Another model was also fitted to a roughness profile from an abnormal situation, to be used during the simulations as representative of such situations:

$$\begin{aligned} A(q) &= 1 - 1.002\, q^{-1} + 0.16\, q^{-2} \\ C(q) &= 1 + 0.5168\, q^{-1} + 0.1035\, q^{-2} \\ \sigma_e^2 &= 2.3420 \end{aligned} \tag{12}$$

Data generated using models (11) and (12) were filtered before entering in our simulations, in order to reproduce exclusively phenomena in the roughness scales, $J_{Rog} = \{1-6\}$.

As for waviness phenomena (W), both the type of waveforms typically found when "piping streaks" are present, as well as other lower frequency irregularities and normal operation conditions profiles were simulated through the superposition (sum) of several sinusoidal waveforms, $W = \sum_{i=1}^{n_W} W_i\left(\lambda_i, A_i\right)$, each one with its own wavelength (λ_i) and amplitude (A_i). We have used four of such elementary waves ($n_W = 4$) to synthesize the overall waviness profiles, through the following sequence of steps:

1. Definition of simulation parameters, including average wavelength ($\bar{\lambda}$), wavelength half range ($\Delta\lambda$), average maximum amplitude ($\bar{A}_{\max}$) and amplitude range ($\Delta A_{\max}$).
2. Generate the wavelengths λ_i for each component wave W_i, where $\lambda_i \sim U\left(\bar{\lambda}-\Delta\lambda, \bar{\lambda}+\Delta\lambda\right)$, i=1:4; with $U(\cdot)$ representing an uniform distribution in the range specified as argument.
3. Generate the amplitude $A_{\max}$ for the final waveform W, where $A_{\max} \sim U\left(\bar{A}_{\max}-\Delta\bar{A}_{\max}, \bar{A}_{\max}+\Delta\bar{A}_{\max}\right)$.
4. Definition of amplitudes for each component wave, W_i, calculating first the unscaled amplitude for each component, A_i^*, and then scaling the four components in order to obtain a final waveform with the amplitude specified in step 3, i.e. $A_i^* \sim U\left(\bar{A}_{\max}-\Delta\bar{A}_{\max}, \bar{A}_{\max}+\Delta\bar{A}_{\max}\right)$, $A_i = A_i^* A_{\max} / \sum A_i^*$.
5. Generation of individual wave components using the same sampling spacing and number of points as for the real profiles ($8.93\ \mu$m and 6144, respectively), and summation to obtain the resulting waviness profile, $W = \sum_{i=1}^{4} W_i\left(\lambda_i, A_i\right)$.

Finally, both the roughness and waviness profiles are combined to obtain the simulated raw profiles, P ($P = R + W$). Our MS-SPC approach was tested under several scenarios, in order to assess its potential to detect shifts of different magnitude in the waviness profile, as well as shifts in roughness. Figure 4 presents the MS-SPC control charts for data regarding five simulation scenarios, described in Table 1.

Table 1. Simulation parameters associated with the different scenarios studied.

Scenario/ Simulation parameter	$\bar{\lambda}$ (mm)	$\Delta\lambda$ (mm)	$\bar{A}_{\max}$ (μm)	$\Delta A_{\max}$ (μm)	*Roughnes s model*
1. Normal operation	40	10	30	20	(3.4)
2. "Piping streaks", moderate magnitude	17	3	70	20	(3.4)
3. "Piping streaks", high magnitude	17	3	110	20	(3.4)
4. "Cockling", high magnitude	80	20	100	20	(3.4)
5. Roughness, high magnitude	40	10	30	20	(3.5)

The first two plots (a and b) refer to control charts for roughness and waviness, respectively, with 99% control limits established after a preliminary Gaussian kernel density estimation step, where 40 samples representing normal operation conditions were used, whereas plot c) combines them into a single plot (lines in this plot are control limits for each parameter, represented only for reference, not aiming to define the combined 99% control region, although this could also be done within the scope of non-parametric approaches [26]). The non-parametric estimation approach was adopted, in order to overcome the difficulties raised by the shapes of the distributions found for the monitoring statistics, that do not resemble any known probability density function. Under such circumstances, the Gaussian kernel density method provides an adequate way to estimate the underlying distribution, through an adequate fit/ smoothness trade-off [36].

From Figure 4 (.a and .b), we can verify that all the shifts simulated under conditions 2-5 are clearly detected in the appropriate control chart, even the one for the moderate "piping streaks" irregularity. In Figure 4.c, one can notice an overlapping occurring in the region of significant waviness phenomena, where "piping streaks" of different magnitude and "cockling" appear superimposed. However, since the former has a quite localized behaviour in the frequency domain, these two types of phenomena can be quite well resolved in the current simulation conditions, by bringing in an extra classifying element, which is the (finite) wavelength where the waviness profile power spectra reaches its maximum, $\lambda_{\max}$.

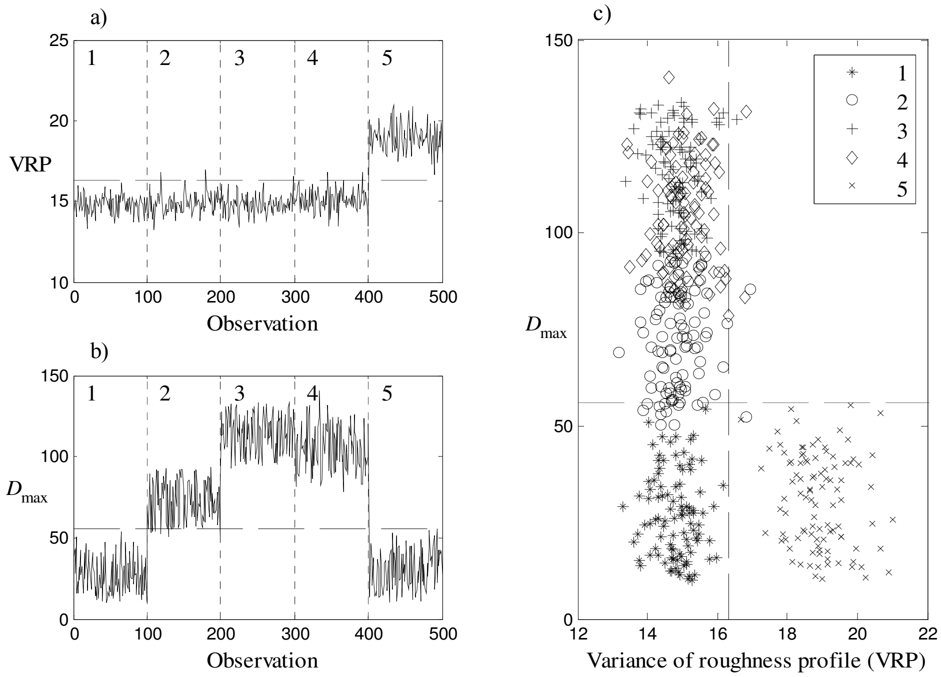

Figure 4. Control charts for monitoring roughness (a) and waviness (b), both with 99% upper control limits, and a combined plot that monitors both statistics (c). The five sectors indicated in plots a) and b) and the symbols used in plot c) refer to the simulation scenarios described in Table 1.

Figure 5 presents such a plot, where we can see that a separation is indeed possible between these two phenomena (Figure 4.c is just the orthogonal projection of the points in this three-dimensional plot, onto the "variance of roughness profile" *versus* "$D_{\max}$" plane). As we are particularly concerned with following "piping streaks", we will pursue this idea a bit further in order to develop a plot that indicates when such phenomena might be occurring, to be presented in the next subsection.

4.2. MS-SPC of Real Paper Surface Profiles

To further test our MS-SPC approach under conditions even closer to those found in real industrial practice, a pilot study was run in the context of a collaboration between our research group and Portucel (a major Portuguese pulp and paper company). Approximately one hundred profiles were gathered, containing samples within the normal operation quality standards as well as others corresponding to several types of abnormal situations. Table 2 presents a general description of the samples whose profiles were used in this study.

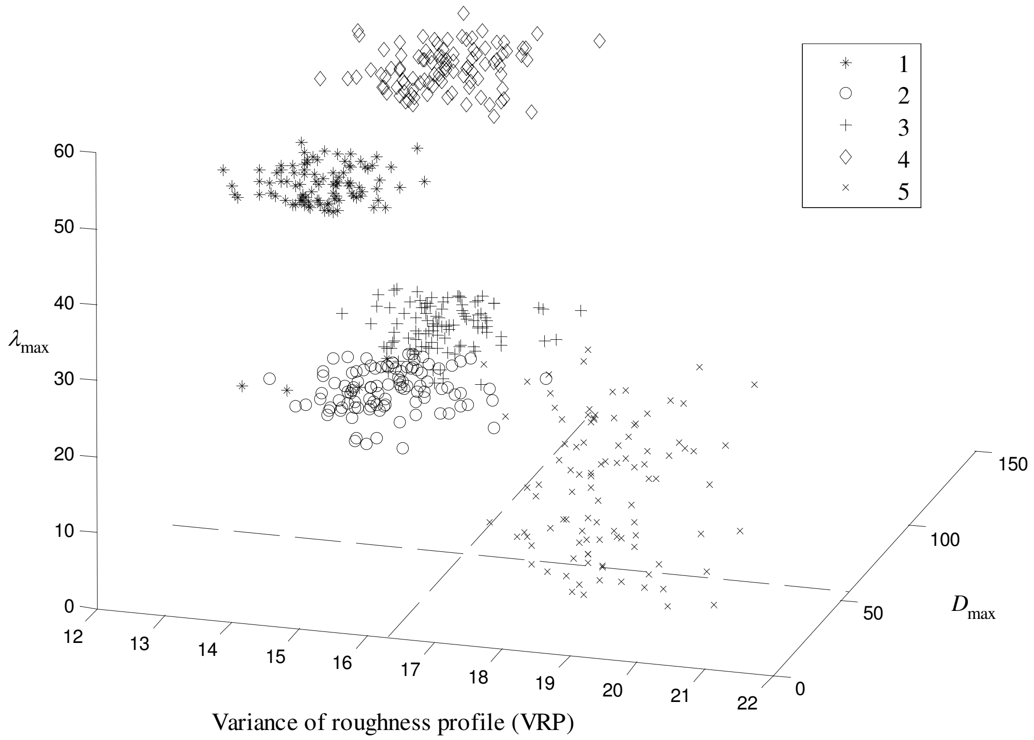

Figure 5. A three dimensional plot of the variance of roughness profiles *versus* Dmax and λ_{max}. Symbols refer to the scenarios described in Table 1. Waviness (2-3) and cockling (4) clusters appear now quite well separated.

Table 2. Description of surface phenomena exhibited by real surface profiles.

Description	*Samples*
Reference set	1-40
No waviness	41-61
Moderate waviness	62-82
High waviness	83-88
Upward trend on Bendtsen roughness	89-98

Control limits were set based on the variability exhibited by the samples from the reference set, following the same approach used for the simulation study. The test set contains samples with low, moderate and high waviness, as well as samples that correspond to an upward trend in roughness magnitude, as measured by the Bendtsen tester [18,40], an instrument based on the air-leakage principle, that measures the volume of air flowing between a ring and the paper surface. As no roughness measurements were available for the former samples, with various levels of waviness magnitude, it is not possible to analyse the monitoring performance of the roughness chart for such samples. Some moderate and high waviness samples can be classified into typical “piping-streaks” and “cockling” representatives by looking at their profiles, but for others that is not possible, and we refer to them simply as (high or moderate) waviness samples.

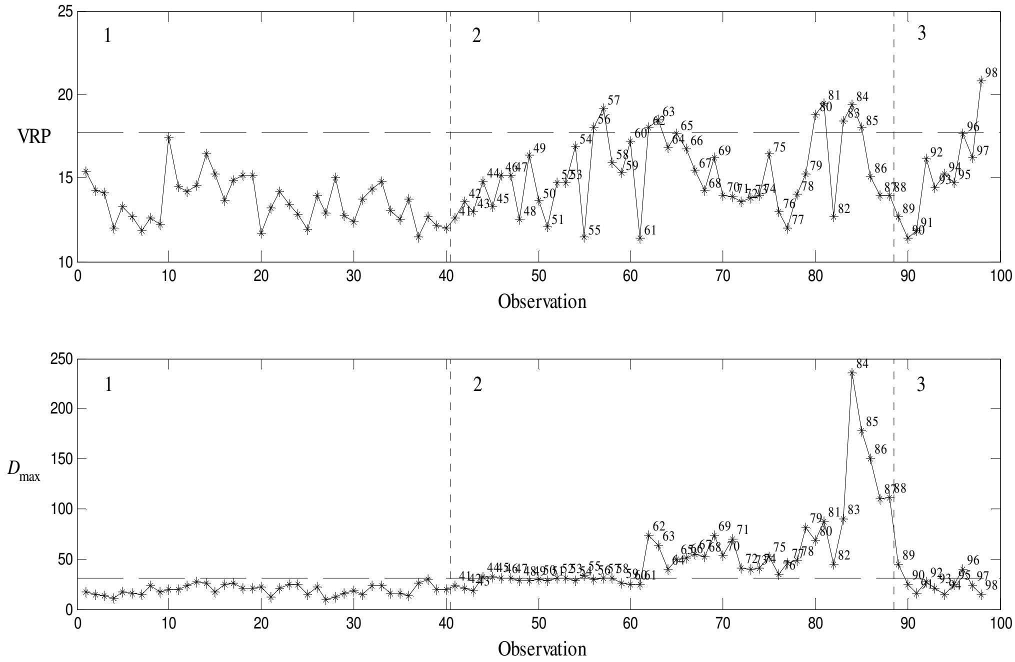

Figure 6. Control charts for monitoring roughness (a) and waviness (b). The first part of the data sets (1) regards reference data, the second (2) is relative to waviness phenomena with different magnitudes (see Table 2 for details) and the third (3) regards an upward trend in roughness, as measured by the Bendtsen tester.

Figure 6 presents our MS-SPC monitoring results for the real profiles. We can see that the SPC chart for monitoring waviness does indeed follow the magnitude trends of the samples described in Table 2. As for the chart relative to roughness, we can also verify that it captures the upward trend in the last 10 samples, besides other significant events scattered through other samples in the test set. To facilitate the detection of samples with “piping streaks” waviness, a two-dimensional plot of $\lambda_{\max}$ *versus* $D_{\max}$, presented in Figure 7 was adopted, where the samples appear segregated along the vertical direction according to the magnitude of the waviness phenomena, and, along the horizontal direction, according to their characteristic wavelength. In general, this plot enables a correct separation, especially when samples present a well defined waviness behaviour, such as is usually the case when “piping streaks” occur. The horizontal classification boundaries presented in Figure 7 were set by analysing the location and localization of the samples classified into three waviness magnitudes classes, through a simple procedure that weights the natural upper and lower boundaries for each adjacent class, using the number of elements in each class, whereas the vertical classification line was drawn using engineering knowledge regarding “piping streaks”.

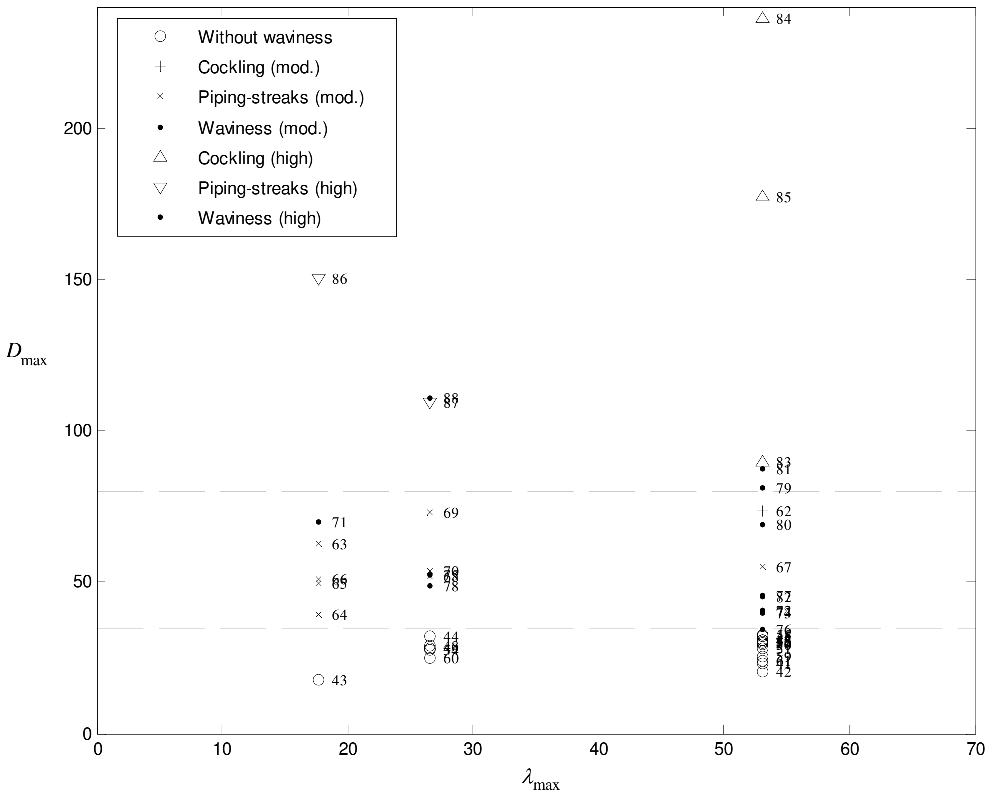

Figure 7. Two-dimensional plot of λ_{max} *versus* D_{max} for the real profiles data set. In this plot, waviness phenomena are classified into three levels of magnitude, separated by horizontal lines (low at the bottom, moderate at the middle and high at the top), and in two regions of characteristic wavelength, the range at the left being characteristic of "piping streaks" phenomena.

From what was presented in these two studies, we can see that the proposed MS-SPC methodology can indeed be used for monitoring simultaneously both paper waviness and roughness phenomena.

5. Conclusions

In this paper a MS-SPC approach for the simultaneous monitoring of both roughness and waviness paper surface phenomena in an integrated way was proposed, and its potential analysed through simulated realistic scenarios and using real industrial data. This approach is built around a wavelet based multiscale decomposition framework that essentially conducts a multiscale filtering of the raw profile, effectively separating the two phenomena under analysis, making also use of available engineering knowledge and information derived from the analysis of the distributions of different quantities through the scales. The results presented from the two case studies carried out allow us to conclude in favour of the adequacy of adopting the proposed MS-SPC for monitoring simultaneously both types of phenomena, but its thorough characterization in terms of Phase 2 detection performance metrics (ARL, ATS) is deferred until more process data can be accumulated, and thus support more detailed statistical modelling.

Acknowledgements

The authors would like to acknowledge collaboration from Portucel, SA and Eng. Dina Angélico (GEPSI – PSE group), and financial support from the Portuguese Foundation for Science and Technology (project POCTI/EQU/47638/2002).

References

1. Bakshi, B. R. (1998). Multiscale PCA with Application to Multivariate Statistical Process Control. *AIChE Journal*, 44(7), 1596-1610.
2. Bakshi, B. R. (1999). Multiscale Analysis and Modeling Using Wavelets. *Journal of Chemometrics*, 13, 415-434.
3. Bernié, J. P., Pande, H., and Gratton, R. (2004). A New Wavelet-Based Instrumental Method for Measuring Print Mottle. *Pulp & Paper Canada*, 105(9), 24-26.
4. Bharati, M. H. and MacGregor, J. F. (1998). Multivariate Image Analysis for Real-Time Process Monitoring and Control. *Industrial & Engineering Chemistry Research*, 37, 4715-4724.
5. Bouydain, M., Colom, J. F., and Pladellorens, J. (1999). Using Wavelets to Determine Paper Formation by Light Transmission Image Analysis. *Tappi Journal*, 82(7), 153-158.
6. Box, G. E. P., Jenkins, G. M., and Reinsel, G. C. (1994). *Time Series Analysis - Forecasting and Control*, 3rd edition. Prentice Hall, Upper Saddle River, NJ.
7. Burrus, C. S., Gopinath, R. A., and Guo, H. (1998). *Introduction to Wavelets and Wavelet Transforms - A Primer*. Prentice Hall, New Jersey.
8. Costa, R., Angélico, D., Saraiva, P., Reis, M., Ataíde, J., Abreu, C., and Bogas, D. (2004). Paper Superficial Waviness: Conception of a Statistical Measurement System. *CAC-2004 Chemometrics in Analytical Chemistry* Lisbon (Portugal).
9. Dai, X. D., Motard, R. L., Joseph, B., and Silverman, D. C. (2000). Corrosion Process Monitoring Using Wavelet Analysis. *Industrial & Engineering Chemistry Research*, 39, 1256-1263.
10. Dijkerman, R. W. and Mazumdar, R. R. (1994). Wavelet Representations of Stochastic Processes and Multiresolution Stochastic Models. *IEEE Transactions on Signal Processing*, 42(7), 1640-1652.
11. Forseth, T. and Helle, T. (1996). Principles and Application of a Method for Assessing Detailed Paper Surface Topography. *82nd Annual Meeting, Technical Session, CPPA*.
12. Fourie, S. H. and de Vaal, P. (2000). Advanced Process Monitoring Using an On-Line Non-Linear Multiscale Principal Component Analysis Methodology. *Computers and Chemical Engineering*, 24, 755-760.
13. Ganesan, R., Das, T. K., and Venkataraman, V. (2004). Wavelet Based Multiscale Process Monitoring - A Literature Review. *IIE Trans. on Quality and Reliability Eng.*, 36(9), 787-806.
14. ISO (1997). *ISO 4287: 1997. Geometrical Product Specifications (GPS) - Surface texture: Profile method - terms, definitions and surface texture parameters.*
15. Jeong, M. K., Lu, J.-C., Huo, X., Vidakovic, B., and Chen, D. (2004). Wavelet-Based Data Reduction Techniques for Process Fault Detection, Georgia Institute of Technology, School of Industrial and Systems Engineering, Statistics Group. (Rep. nb. 11/2004).
16. Jin, J. and Shi, J. (1999). Feature-Preserving Data Compression of Stamping Tonnage

Information Using Wavelets. *Technometrics*, 41(4), 327-339.

17. Jin, L. and Shi, J. (2001). Automatic Feature Extraction of Waveform Signals for In-Process Diagnostic Peformance Improvement. *Journal of Intelligent Manufacturing*, 12, 257-268.

18. Kajanto, I., Laamanen, J., and Kainulainen, M. (1998). Paper Bulk and Surface. *Paper Physics* (Edited by K. Niskanen), 88-113. Fapet Oy.

19. Kano, M., Nagao, K., Hasebe, S., Hashimoto, I., Ohno, H., Strauss, R., and Bakshi, B. R. (2002). Comparison of Multivariate Statistical Process Monitoring Methods with Applications to the Eastman Challenge Problem. *Computers and Chemical Engineering*, 26, 161-174.

20. Kortschot, M. T. (1997). The Role of the Fibre in the Structural Hierarchy of Paper. *The Fundamentals of Papermaking Materials - Transactions of the 11th Fundamental Research Symposium*, 351-399.

21. Lada, E. K., Lu, J.-C., and Wilson, J. R. (2002). A Wavelet-Based Procedure for Process Fault Detection. *IEEE Transactions on Semiconductor Manufacturing*, 15(1), 79-90.

22. Ljung, L. (1999). *System Identification - Theory for the User*, 2nd edition. Prentice Hall, Upper Saddle River, NJ.

23. MacGregor, M. A. (2001). Some Impacts of Paper Making on Paper Structure. *Paper Technology*, 42(3), 30-44.

24. Mallat, S. (1989). A Theory for Multiresolution Signal Decomposition: The Wavelet Representation. *IEEE Transaction on Pattern Analysis and Machine Intelligence*, 11(7), 674-693.

25. Mallat, S. (1998). *A Wavelet Tour of Signal Processing*. Academic Press, San Diego.

26. Martin, E. B. and Morris, A. J. (1996). Non-Parametric Confidence Bounds for Process Performance Monitoring Charts. *Journal of Process Control*, 6(6), 349-358.

27. Misra, M., Yue, H. H., Qin, S. J., and Ling, C. (2002). Multivariate Process Monitoring and Fault Diagnosis by Multi-Scale PCA. *Computers and Chemical Engineering*, 26, 1281-1293.

28. Montgomery, D. C. (2001). *Introduction to Statistical Quality Control*, 4th edition. Wiley, New York.

29. Nomikos, P. and MacGregor, J. F. (1995). Multivariate SPC Charts for Monitoring Batch Processes. *Technometrics*, 37(1), 41-59.

30. Nomikos, P. and MacGregor, J. F. (1995). Multi-Way Partial Least Squares in Monitoring Batch Processes. *Chemometrics and Intelligent Laboratory Systems*, 30, 97-108.

31. Nordström, J.-E. P., Lindberg, S., and Lundström, A. (2002). Human Perception and Optical Measurement of HSWO Waviness. *IPGAC (International Printing & Graphic Arts Conference)* Bordeaux, France.

32. Rioul, O. and Vetterli, M. (1991). Wavelets and Signal Processing. *IEEE Signal Processing Magazine*, 8(4), 14-38.

33. Sahni, N. S., Aastveit, A. H., and Naes, T. (2005). In-Line Process and Product Control Using Spectroscopy and Multivariate Calibration. *Journal of Quality Technology*, 37(1), 1-20.

34. Sander, M. (1991). *A Practical Guide to the Assessment of Surface Texture*. Feinprüf Perthen GmbH, Göttingen.

35. Shao, R., Jia, F., Martin, E. B., and Morris, A. J. (1999). Wavelets and Non-Linear Principal Components Analysis for Process Monitoring. *Control Engineering Practice*, 7, 865-879.

36. Silverman, B. W. (1986). *Density Estimation for Statistics and Data Analysis*. Chapman and Hall, London.

37. Sze, D. H. and Waech, T. G. (1997). Paper Waviness and Finer Alignement Streaks in Paper Forming. *CPPA Annual Technical Meeting Proceedings* Montréal, Canada.

38. Top, S. and Bakshi, B. R. (1998). Improved Statistical Process Control Using Wavelets. *Foundation of Computer Aided Process Operations FOCAPO 98*, 332-337.

39. Trygg, J., Kettaneh-Wold, N., and Wallbäcks, L. (2001). 2D Wavelet Analysis and Compression of On-Line Industrial Process Data. *Journal of Chemometrics*, 15, 299-319.

40. Van Eperen, R. H. (1991). *Paper Properties and Testing Procedures*, 3rd edition. Vol. 7, *Pulp and Paper Manufacture*. The Joint Textbook Committee of The Paper Industry, Atlanta.

41. Vetterli, M. and Kovačević, J. (1995). *Wavelets and Subband Coding*. Prentice Hall, New Jersey.

42. Wågberg, P. and Johansson, P.-Å. (2002). Characterization of Paper Surfaces Using Optical Profilometry. In *Handbook of Physical Testing of Paper*, 2nd ed. (Edited by J. Borch, M. B. Lyne, R. E. Mark, and C. C. Habeger, Jr.), Marcel Dekker.

43. Westerhuis, J. A., Kourti, T., and MacGregor, J. F. (1999). Comparing Alternative Approaches for Multivariate Statistical Analysis of Batch Process Data. *Journal of Chemometrics*, 13, 397-413.

44. Woodall, W. H., Spitzner, D. J., Montgomery, D. C., and Gupta, S. (2004). Using Control Charts to Monitor Process and Product Quality Profiles. *Journal of Quality Technology*, 36(3), 309-320.

45. Zhao, Z., Jin, Y., and Wang, J. (2000). Application of Wavelet Transform to Process Operating Region Recognition. *Journal of Chemical Engineering of Japan*, 33(6), 823-831.

Authors' Biographies:

Marco S. Reis is a Teaching Assistant and PhD Student at the Department of Chemical Engineering of the University of Coimbra, Portugal. He has worked several years in the Product Development Department of a major Portuguese pulp and paper company and his current research interests are centred around the areas of Process Systems Engineering, Applied Statistics and Chemometrics. He is an elected member of ENBIS Council and author or co-author of several articles and conference presentations in the fields of Process Systems Engineering, Applied Statistics and Chemometrics.

Pedro M. Saraiva is an Associate Professor in the Department of Chemical Engineering and Pro-Rector of the University of Coimbra, Portugal. His interests are in the areas of Process Systems Engineering and Quality Management. He is a senior member of ASQ and received from this society the Feigenbaum Award (1998). He is the Founder and Partner of QUAL-Quality Management Consulting Firm, author and co-author of several books, articles and conference presentations in the fields of Process Systems Engineering and Quality Management.